frontiers in Earth Science

ORIGINAL RESEARCH
published: 01 October 2021
doi: 10.3389/feart.2021.721724

Hydrological Evolution of a Lake Recharged by Groundwater in the Badain Jaran Desert Over the Past 140 years

Gaolei Jiang[1,2,3], Nai'ang Wang[1]*, Xin Mao[2,3], Hua Zhao[2,3], Linjing Liu[2,3], Jianmei Shen[2], Zhenlong Nie[2] and Zhe Wang[2]*

[1]Centre for Glacier and Desert Research, College of Earth and Environmental Sciences, Lanzhou University, Lanzhou, China, [2]Institute of Hydrogeology and Environmental Geology, Chinese Academy of Geological Sciences, Shijiazhuang, China, [3]Key Laboratory of Quaternary Chronology and Hydro-Environmental Evolution, China Geological Survey, Shijiazhuang, China

OPEN ACCESS

Edited by:
Zhiwei Xu,
Nanjing University, China

Reviewed by:
José Darrozes,
UMR5563 Géosciences Environnement Toulouse (GET), France
Li Wu,
Anhui Normal University, China
Steffen Mischke,
University of Iceland, Iceland

***Correspondence:**
Gaolei Jiang
jianggl198899@163.com
Nai'ang Wang
wangna@lzu.edu.cn

Specialty section:
This article was submitted to Quaternary Science, Geomorphology and Paleoenvironment, a section of the journal Frontiers in Earth Science

Received: *07 June 2021*
Accepted: *23 August 2021*
Published: *01 October 2021*

Citation:
Jiang G, Wang N, Mao X, Zhao H, Liu L, Shen J, Nie Z and Wang Z (2021) Hydrological Evolution of a Lake Recharged by Groundwater in the Badain Jaran Desert Over the Past 140 years. Front. Earth Sci. 9:721724. doi: 10.3389/feart.2021.721724

Understanding the evolution of lakes in arid areas is very important for water resource management. Previous studies have mainly focused on lakes with runoff recharge, while the evolution of groundwater recharge lakes in hyper-arid areas is still less known. In this study, an 86 cm-long sediment core was extracted from Sayinwusu Lake, one of groundwater-recharge lakes in the southeastern Badain Jaran Desert, Northwest China. ^{210}Pb and ^{137}Cs dating, total organic carbon (TOC) and total nitrogen (TN) contents, and mineral content analysis were used to reconstruct the lake evolution over the past 140 years. The evolution of Sayinwusu Lake since 1880 can be divided into two periods. In the first period from 1880 to 1950, the TOC and TN contents were low, and the minerals consisted of all detrital minerals, which indicate that the lake's primary productivity and salinity were low. During the second period from 1950 to 2018, the contents of TOC, TN, and carbonate minerals increased rapidly at the beginning of the 1950s, indicating that the lake's primary productivity and salinity increased. Comprehensive analysis of regional climate data suggests that the increase in evaporation caused by rising temperature is an important factor affecting lake evolution in the desert. Although precipitation has increased in the arid region of Northwest China in recent decades with increasing temperature, the enhancement of the evaporation effect is much greater. As a record from groundwater recharge lakes in deserts, our study provides new insight into projecting future lake changes in hyper-arid areas.

Keywords: lake evolution, groundwater recharge, global warming, evaporation, arid areas

INTRODUCTION

Lakes are important water resources, especially in hyper-arid areas. Understanding lake evolution patterns can help us predict lake development trends and manage water resources (Panizzo et al., 2013; Creutz et al., 2016; Lopez et al., 2019; Wan et al., 2019; Woolway et al., 2020). Previous studies of lake evolution have mainly focused on the important role of runoff, precipitation, and/or snow melt water in hydrological systems (Zhai et al., 2011; Long et al., 2012; Liu et al., 2013; Li et al., 2016). In hyper-arid areas, including Xinjiang Province and Gansu Province, recharge by groundwater plays a crucial role in the evolution of the main inland basin and is at least equal to, if not greater than, the

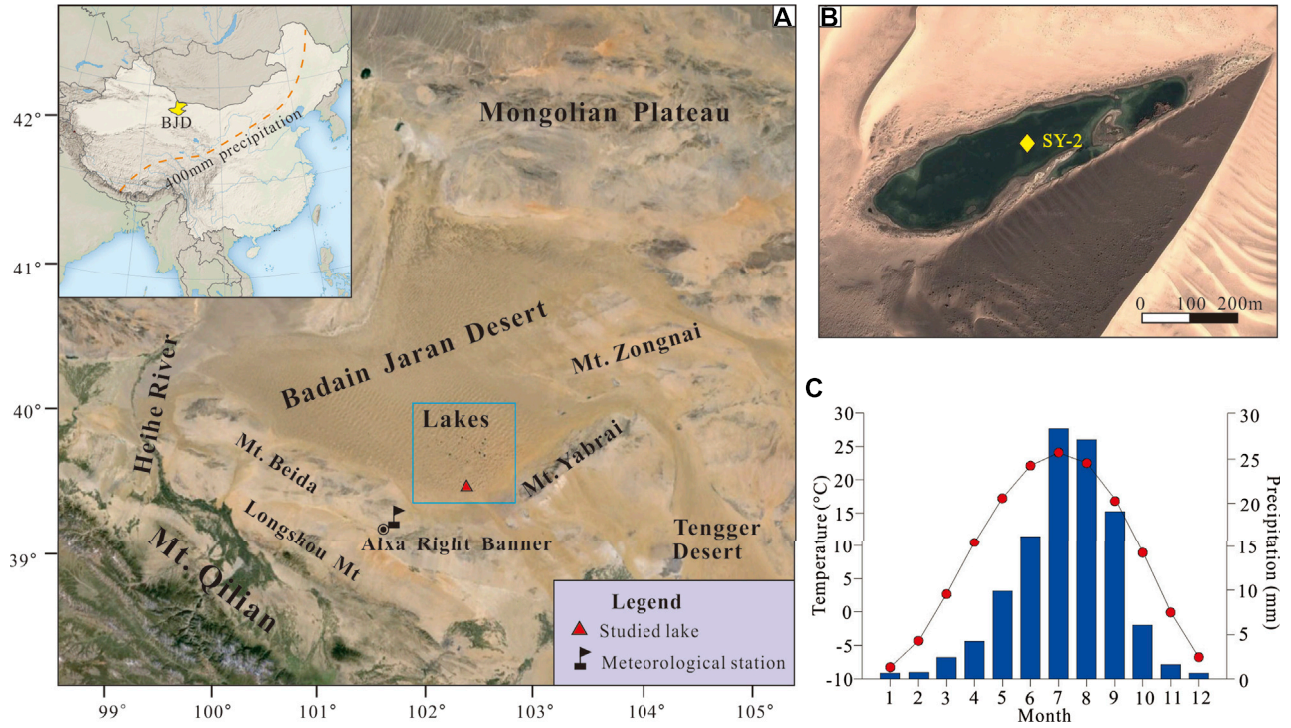

FIGURE 1 | Sketch map showing the geographic setting of the BJD **(A)**, the location of the SY-2 sediment core from Sayinwusu Lake **(B),** and the variation in monthly temperature (red circles) and precipitation (blue pillars) [**(C)**, data are the averages for 1960–2017].

amount of runoff and precipitation (Zhang and Li, 2005a; Zhang and Li, 2005b). The evolution of lakes recharged by groundwater is characterized by intense vertical intersphere water recharge from other areas and no discharge except evaporation; this situation is different from the previous lake evolution model. Many studies have been conducted and have achieved much progress on the evolution pattern, driving factors of lake evolution, and response to climate change for lakes recharged by runoff and/or precipitation (Chen et al., 2009; Long et al., 2012; Liu et al., 2013; Wang et al., 2014; Wu et al., 2020; Fu et al., 2021). However, much less work has been done on the evolution of groundwater recharge lakes.

The Badain Jaran Desert (BJD), located in western Inner Mongolia in a hyper-arid area of China, is sensitive to climate change, with an increase in the temperature of 0.34°C per decade (**Figure 1**; Yang et al., 2011; Ning et al., 2021). The BJD, with an area of 5.2 × 104 km^2, is the second largest desert in China (Zhu et al., 2010). It is characterized by the coexistence of more than 110 perennial lakes and thousands of mega-dunes (Dong et al., 2013). The BJD has the tallest mega-dunes on Earth, with mega-dunes more than 100 m tall covering 68% of the area and concentrated in the southeastern part of the sand sea (Dong et al., 2013). More than 90% of the recharge of lakes between mega-dunes is from groundwater (Dong et al., 2016; Wang et al., 2016). Therefore, the BJD is an ideal region to study the evolution pattern of lakes recharged by groundwater. Previous studies in the BJD were mainly based on the dating of discontinuous lake sediments during the late Quaternary, especially the Holocene at the millennial scale (Yang and Williams, 2003; Yang et al., 2010; Bai et al., 2011; Wang et al., 2016; Chen et al., 2019). This is not sufficient for a detailed understanding of the factors influencing lake evolution during past decades, which is important for predicting the development trend in future decades or centuries.

The global environment has experienced dramatic change, with the highest rate of increase in global temperature over the last century (Woolway et al., 2020). Arid zones are recognized to be more sensitive than other areas to temperature variations associated with global climate change (Huang et al., 2016), and the resulting changes in evaporation are an important factor in lake evolution (Li et al., 2016; Wang et al., 2016). Therefore, the past century is a key period for understanding lake evolution and predicting its trend in the context of global warming (Neukom et al., 2019). Unfortunately, few studies on lake evolution have been conducted during this period in the BJD. In this study, we reconstructed the lake evolution history over the last 140 years based on continuous lake sediments, which may provide new insight into projecting the trend of lake evolution responses to future climate change.

STUDY AREA

The BJD is located on the northwestern Alxa Plateau in Northwest China (**Figure 1A**). It has an elevation of 900–1800 m a.s.l., falling from the southeast to the northwest.

To the south, it is bounded by the Beida Mountains (Mt) and the Heishantou Mt (maximum elevation 1963 m a.s.l.), which separate it from the Gobi of the Hexi Corridor (Dong et al., 2013). To the southeast, it is bounded by the Yabrai Mt (maximum elevation 1957 m a.s.l.), which separate it from the Tengger Desert. To the west and northwest, it stretches down to Ugrian Lake and the Heihe River. To the north, it is bounded by Guaizi Lake, close to the Mongolian Gobi (Dong et al., 2013). Stratigraphic studies of the Badain Jaran Basin demonstrate that Cretaceous strata are widely distributed in the piedmont area of the surrounding mountains and the Badain Jaran Desert. They are several thousand metres thick and mainly consist of red and brick-red sandstone, siltstone with calcareous nodules intercalated with a small amount of conglomerate, and calcareous sandstone (BGMIMAR, 1991). Cenozoic sediments are distributed in the western and southern intermontane areas, which unconformably underlie the upper Quaternary deposits and are less than 200 m thick. The Quaternary aeolian sand has a thickness of 200–400 m and is intercalated with several lacustrine layers (Wang et al., 2015a). Studies have assumed that the sandy materials in the Badain Jaran should have been derived from the weathered extensive lacustrine sediments of dry lake beds in the west and northwest (Yang, 1991; Yan et al., 2001) and the giant alluvial fan of the Heihe River (Mischke, 2005; Hu and Yang, 2016).

The lakes lying among mega-dunes are concentrated within an area of approximately 4,000 km^2 (Dong et al., 2013). Most lakes are less than 0.6 km^2, and the largest is 1.46 km^2. Water depth is generally a few metres up to 10 m, and the deepest lake depth is 15.9 m (Zhang et al., 2013; Wang et al., 2016). The hydrological properties of the lakes vary greatly, with the total dissolved solids (TDS) ranging from less than 1 to 400 g/L (Yang and Williams, 2003; Lu et al., 2010). Most lakes from the southeast edge to the hinterland are of the sulfate–carbonate–chloride type with increasing salinity (Lu et al., 2010). Although the origin of groundwater in the desert remains a hotly debated issue, it is generally agreed that groundwater is the main water source of the lakes and is primarily from the south and southeast areas, such as the Yabrai Mt, and Qilian Mt (Ma and Edmunds, 2006; Gates et al., 2008a; Dong et al., 2013; Wang et al., 2016).

The BJD has an extreme continental desert-type climate (Dong et al., 2004). The mean precipitation ranges from 40 to 90 mm, decreasing from the southeast to the northwest. Most of the precipitation occurs in summer (**Figure 1C**). The evaporation from lake surfaces is 1,450 mm, which is more than 20 times the amount of precipitation (Hu et al., 2015). The mean annual air temperature ranges from 9.5 to 10.3°C, with the lowest monthly mean temperature of 8.3°C in January and the highest of 24.1°C in July (**Figure 1C**). The mean annual wind speed ranges from 2.8 to 4.6 m s^{-1}, and the wind direction is mainly northwest (Hu and Yang, 2016).

The surface vegetation coverage of the BJD ranges from 5 to 50, with most areas having very low coverage; the vegetation is dominated by xerophytic and ultraxerophytic shrubs and subshrubs, and herbacea is dominated by annual plants. On the sandy hills, the vertical distribution of vegetation is obvious. In the dry lake basin, the *Nitraria tangutorum* community is widely distributed, accompanied by *Zygophyllum xanthoxylum* and *Calligonum mongolicum* (Cui et al., 2014; Wang et al., 2015b). Around the modern lake shore, the vegetation is distributed in a ribbon with a width of a few metres to a dozen metres. Along the lake, there is a marsh-shaped halophytic meadow, mainly composed of *Trigolochin maritimum, Glaux maritima*, and *Aeluro littorlis*. In the periphery, there is a halophytic meadow, mainly composed of *Phragmites communis* and *Achnatherum splendens*. Due to the government's relocation policy and the improvement of living conditions, there are only a few herders living around a few lakes. In 2009, the BJD became a global desert geopark, and thousands of people visited it every year, mainly in October.

The distribution of lakes in the BJD is relatively concentrated in the southeastern region. Lakes with lower salinities are more sensitive to the environmental changes and are easily observed for hydrochemical changes. Sayinwusu Lake, located at the southeastern margin of the BJD, has an area of approximately 0.12 km^2 (**Figure 1B**). The lake is 720 m long and 170 m at the widest point, with the largest water depth of approximately 2 m. The lake water has a pH of 9.5 and salinity of 18.0 g/L with major cations of K^+ (384 mg/L), Na^+ (5,330 mg/L), Ca^{2+} (37 mg/L), and Mg^{2+} (751 mg/L) and major anions of Cl^- (6,440 mg/L), SO_4^{2-} (4,166 mg/L), HCO_3^- (693 mg/L), and CO_3^{2-} (531 mg/L) (team unpublished data). Due to the high salinity, there are no fish in the lake, and no animals, such as camels, drink the lake water. Terrestrial vegetation is distributed in belts around the lake shores, with areal extents of tens of metres. The dominant plant species around the lake are mainly xerophytes, super-arid shrubs, and semi-shrubs, and are mainly composed of *Trigolochin maritimum, Glaux maritima, and Aeluro littorlis* inside and *Phragmites communis* and *Achnatherum splendens* outside.

MATERIALS AND METHODS

Field Sampling

An 86 cm long sediment core (SY-2) was drilled from the centre of Sayinwusu Lake (102°19.82′ E, 39°34.00′ N) in September 2018 A.D. using a gravity corer. The water depth of the sampling point is approximately 1.6 m. The sediment core was sectioned at 1.0 cm intervals (86 samples) and then fully dried in a vacuum-freezing dryer at −25°C for 48–72 h. Before laboratory analysis, these samples were stored in a dry place at room temperature.

^{210}Pb and ^{137}Cs Dating

Twenty-five subsamples were selected at 2-cm intervals for the upper 50 cm part of the sediment core and were ground to fine powder (< 63 μm) in an agate mortar. The activities of ^{137}Cs, ^{210}Pb, and ^{226}Ra in the samples were determined by a low-background well-type germanium detector (EG and GOrtec Gamma Spectrometry) at the State Key Laboratory of Lake Sciences and Environment, CAS. ^{137}Cs was detected at 662 keV, ^{210}Pb was determined via gamma emission at 46.5 keV, ^{226}Ra was measured at 295 keV, and 352 keV g-rays were emitted by its daughter isotope ^{214}Pb. Standard errors (2σ) were calculated from the counting statistics. The excess ^{210}Pb (^{210}Pbex) activity was calculated by subtracting the activity of ^{226}Ra

from the total ^{210}Pb activity. $^{210}Pb_{ex}$ activity is employed to calculate a chronology using the constant rate of supply (CRS) dating model (Appleby and Oldfield, 1978; Appleby, 2001; Swarzenski, 2014). The calculated equation is as follows:

$$A_h = A_0 e^{-\lambda t},$$

where Ah is the cumulative residual unsupported or excess ^{210}Pb activity beneath sediment of depth h, A_0 is the total unsupported ^{210}Pb activity in the sediment column, λ is the ^{210}Pb decay constant, 0.03114 years^{-1}, and t represents time.

TOC and TN Analysis

Eighty-four subsamples at 1 cm intervals were ground to fine powder (< 63 μm) in an agate mortar, treated with 1 N HCl to remove inorganic carbonates, and then rinsed repeatedly with deionized water to remove soluble salts. The residual samples were dried for measurement. The total carbon and total nitrogen contents were determined by an EA 3,000 elemental analyser at the State Key Laboratory of Lake Sciences and Environment, Chinese Academy of Science (CAS). The repetitive errors were less than 3%. The total organic carbon contents were calculated by subtracting the inorganic carbon contents in carbonates from the total carbon contents.

The total organic carbon (TOC)/total nitrogen (TN) ratios of lacustrine sediments are usually used to evaluate the predominance of autochthonous versus allochthonous sources of organic matter (Meyers, 2003). In general, carbon-to-nitrogen (C/N) ratios less than 10 indicate that the organic matter is from protein-rich and cellulose-poor aquatic organisms (Meyers, 2003), the mean C/N value of benthos is approximately 3, and algae and phytoplankton have values of approximately 5–12 and generally less than 10 (Hedges et al., 2002). However, when the organic matter is from protein-poor and cellulose-rich terrestrial plants, the C/N ratio is greater than 20 (Meyers, 2003).

Mineral Analysis

Eighty-six subsamples at 1 cm intervals were ground to fine powder prior to measurement. The mineralogy was measured at the Key Laboratory of Western China's Environmental Systems (Ministry of Education) by a powder X-ray diffractometer (XRD, PANalytical X'Pert Pro MPD). Each sample was spread and leveled onto a 1.5 cm^2 × 1.5 cm^2 concave glass plate for XRD determinations. XRD employs the radiation of a Cu target at 40 kV and 40 mA to generate X-rays that irradiate a sample at a scanning angle of 2θ (5–75°) with a 0.01° minimum step size and produce the diffraction peaks of the sample. Other equipment settings are automatic variable divergence detector slits. Corundum (α-Al_2O_3) was selected as the internal standard. The compositions of minerals in samples were determined by comparison of the characteristic diffraction peaks with the standard card spectrum using the software X'Pert HighScore Plus. The detailed calculation method of mineral content can be found in Last (2001).

RESULTS

^{210}Pb and ^{137}Cs

In the studied sediment core, the vertical distributions of the activities of ^{210}Pb and ^{137}Cs are shown in **Table 1** and **Figure 2A**. The first appearance of ^{137}Cs activity occurs at a depth of 36 cm with a corresponding activity of 1.83 Bq/kg. The peak of ^{137}Cs activity is identified at a depth of 30 cm with a corresponding activity of 18.47 Bq/kg. Above 30 cm, the ^{137}Cs activity gradually decreased to approximately about 3 Bq/kg (**Figure 2A**). The excess ^{210}Pb ($^{210}Pb_{ex}$) activity in the core decreases from 253.39 Bq/kg at the core surface to near zero at 50 cm depth (**Figure 2A**).

TOC, TN, and TOC/TN

The TOC and TN contents are very low and constant around 0.1% for TOC and ~0.05% for TN, and no clear peak is observed during this period. The C/N ratio is very noisy during this period except for 1885 A.D., where a very strong peak is observed. The TOC content increases rapidly at 40–41 cm (1948–1950 A.D.) and then maintains a higher content (0.40–1.47%), and **Figure 3** shows four main peaks compared to the geochemical background of approximately 0.5% for TOC and 0.15% for TN. These main peaks correspond to the years 1950–1952 (TOC = 0.85%, TN = 0.10%), 1960 (TOC = 0.8%, TN = 0.12%), 1995 (TOC = 1.47%, TN = 0.24%), ~2004–2007 (TOC = 1.13%, TN = 0.18%), and the highest peak (TOC = 2.01%, TN = 0.35%) observed for 2015–2018. Overall, the TOC/TN ratios are less than 10 with an average value of 6.25. The C/N ratio during 1950–2018 decreased slowly from 8 to 5, and the noise strongly decreased compared to the 1880–1950 period (**Figure 3**).

Mineral Variations

The mineral constituents of core SY-2 at 44–85 cm (1880–1944 A.D.) are detrital minerals, including quartz, feldspars, and mica and a small amount of clay minerals, such as chamosite and clinochlore. The upper part (0–40 cm; 1945–2018 A.D.) is still dominated by detrital minerals but is characterized by various carbonates, including monohydrocalcite, calcite, and dolomite and a small amount of halite. In this part, the average content of carbonates is 9.5%, with two higher phases for 29–36 cm (1955–1968 A.D.) with a value 11% and 0–16 cm (1998–2018 A.D.) with a value 13%. In carbonates, monohydrocalcite is predominant, with a maximum content of 26% (**Figure 4**).

DISCUSSION

Core Chronology

The ^{137}Cs activity versus depth shows no tailing effect, indicating that the vertical migration of ^{137}Cs can be neglected in Sayinwusu Lake (Audry et al., 2004). The first appearance of ^{137}Cs activity at a depth of 36 cm can be dated to the early 1950s (most likely 1952 A.D.) (Jin et al., 2010; Liu et al., 2012). The peak of ^{137}Cs activity at a depth of 30 cm is assigned to the maximum atmospheric global fallout corresponding to 1963 A.D. (Robbins and Edgington, 1975). The CRS dating model suggests an age of 1968 (+11/−16) A.D. at 30 cm and an age of 1955 (+16/−33) A.D. at 36 cm (**Figure 2B**). The ^{137} Cs dating yields ages of 1955 A.D. at 36 cm and 1963 A.D. at 30 cm, which is in general agreement with the ^{210}Pb dates. However, the Chernobyl accident in 1986 A.D. is not identified in the studied core, similar to other lacustrine

TABLE 1 | Measured results and standard errors (2σ) for ^{210}Pb and ^{137}Cs dating.

Sample ID	Depth (cm)	Mass depth (g/cm^2)	^{137}Cs (Bq/kg)	Errors (± 2σ)	$^{210}P_{bex}$ (Bq/kg)	Errors (± 2σ)	^{226}Ra (Bq/kg)	$^{210}Pb_T$ (Bq/kg)
SY-2-2	2	0.43	8.52	2.65	253.39	22.60	42.84	296.23
SY-2-4	4	1.21	3.54	1.85	221.00	20.43	35.51	256.51
SY-2-6	6	2.31	2.40	1.22	159.48	12.85	36.30	195.78
SY-2-8	8	3.61	3.22	1.90	148.99	12.04	30.84	179.83
SY-2-10	10	4.96	3.05	2.45	99.54	10.33	32.96	132.50
SY-2-12	12	6.65	5.01	2.84	106.84	10.24	45.12	151.96
SY-2-14	14	7.99	10.88	3.10	54.84	7.67	44.89	99.73
SY-2-16	16	9.29	7.40	2.40	69.47	8.26	44.03	113.49
SY-2-18	18	10.73	5.08	2.14	107.76	10.22	42.91	150.67
SY-2-20	20	11.95	14.91	3.75	74.20	9.65	58.19	132.40
SY-2-22	22	13.53	4.07	1.66	97.94	10.36	35.01	132.96
SY-2-24	24	14.88	14.81	2.78	67.85	8.49	54.98	122.84
SY-2-26	26	16.33	8.09	2.44	78.36	8.69	59.72	138.09
SY-2-28	28	18.03	10.46	2.80	59.49	8.03	43.05	102.54
SY-2-30	30	19.70	18.47	3.51	62.64	8.80	48.31	110.95
SY-2-32	32	21.23	10.54	3.06	38.47	5.05	32.64	71.11
SY-2-34	34	23.02	4.28	1.73	23.32	4.20	34.76	58.07
SY-2-36	36	24.92	1.83	1.41	34.64	5.11	33.92	68.55
SY-2-38	38	26.95	0.00	—	85.83	10.66	34.89	120.72
SY-2-40	40	29.01	0.00	—	14.32	2.87	34.51	48.83
SY-2-42	42	31.91	0.00	—	7.62	2.49	40.44	48.06
SY-2-44	44	34.99	0.00	—	13.15	3.01	35.24	48.38
SY-2-46	46	38.28	0.00	—	12.18	3.33	32.28	44.47
SY-2-48	48	41.92	0.00	—	5.74	2.12	51.04	56.78
SY-2-50	50	45.36	0.00	—	6.74	2.50	41.85	48.60

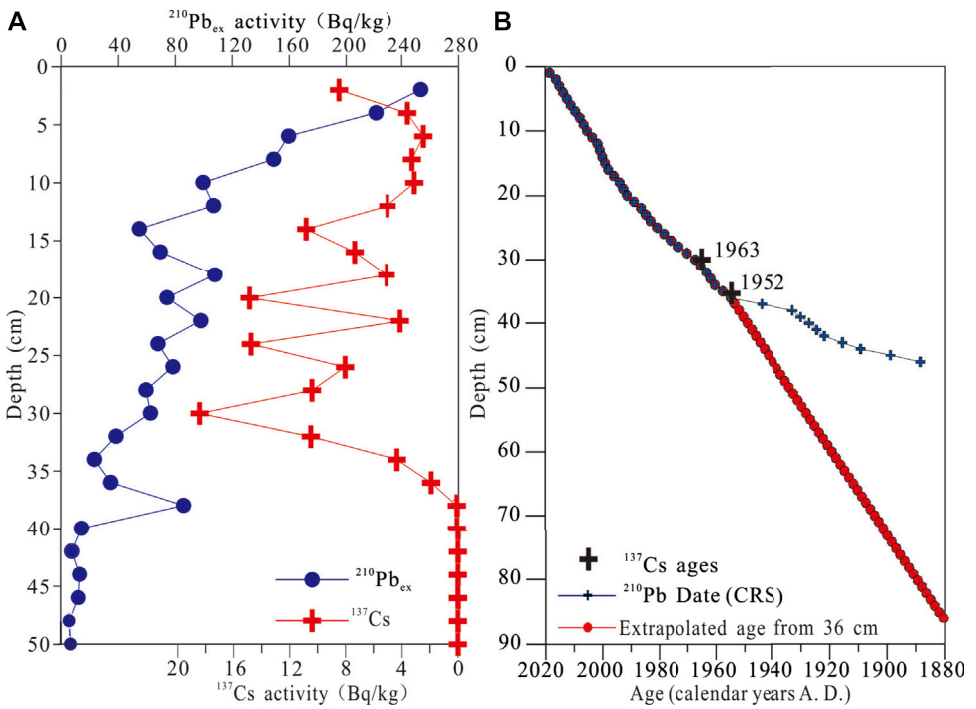

FIGURE 2 | Age model for sediment core SY-2. **(A)** ^{137}Cs and excess ^{210}Pb ($^{210}Pb_{ex}$) activity versus depth. **(B)** Age-depth relation from ^{210}Pb and ^{137}Cs dating.

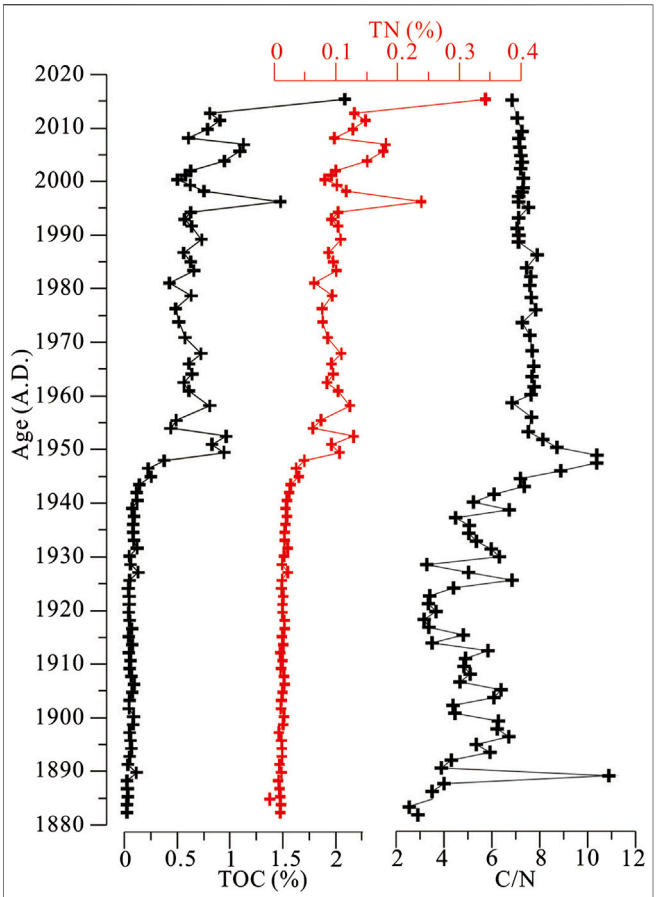

FIGURE 3 | TOC and TN contents and the C/N ratios in sediment core SY-2.

sediment records in China and Japan, because of its small impact on ^{137}Cs activity in these areas (Liu et al., 2012; Zhang et al., 2012).

Based on the CRS dating model, the sedimentation rate decreases below 36 cm (**Figure 2B**). Clearly, this fact does not accord with the lacustrine sedimentary characteristics, which indicates that the chronology of the ^{210}Pb CRS dating model is not reliable in the lower part of the sediment core (> 36 cm, before 1952 A.D.). Considering that: 1) there is no surface runoff recharge to the lakes in the BJD, and more than 90% of the lake recharge depends on groundwater (Dong et al., 2016; Wang et al., 2016); 2) although the lake sediments are from the surrounding aeolian sand, most of the aeolian sand was transported to the lake shore by saltation and creep (Wang et al., 2018), and sand from the shores is eroded by waves and then distributed in the lake (Li et al., 2018); 3) the locations of lakes and mega-dunes are relatively fixed (Yang et al., 2011; Wang et al., 2016); 4) human and animal activities are limited in the desert, so the lake sediment sequence is considered as formed continuously; 5) the ^{210}Pb and ^{137}Cs dating of adjacent lakes indicate that the sediment accumulation rates were relatively stable in the last century (Herzschuh et al., 2006; Liu et al., 2016); and 6) the average content of carbonate is only 9.5% in the upper part of the sediment core SY-2, which has a limited effect on the deposition rate. Therefore, the age of lower sediments (> 36 cm) can be dated by the average mass accumulation rate and that of the upper sediments (< 36 cm) can be determined by the CRS dating model. Finally, the obtained results show that the sediment core covers a period of ~1880–2018 A.D. and that the average sedimentation rate of the upper sediments is 0.57 (+0.19/−0.20) cm/a by CRS age model, which is consistent with those of other lakes in the BJD (Liu et al., 2016).

Proxy Interpretation

TOC, TN, and C/N

The C/N ratios of sediment core SY-2 are less than 10, with an average of 6.25, indicating that the organic matter of these sediments is autochthonous, which is consistent with results from other lakes in the BJD (Dong et al., 2018). The lack of a relationship between TOC and C/N (**Figure 5A**) also suggests that the organic matter of these sediments is autochthonous and reflects primary productivity (Lu and An, 2010). Due to the high salinity, no fish are found in the lake, and no animals, such as camels, drink the lake water. In addition, the administrative region of Alxa Right Banner was established in 1961. Due to government policies and the improvement of living conditions, most herders moved away from the desert in the last 20 or 30 years (based on communications with local herders). Therefore, grazing and local people have little effect on primary productivity. The TOC content reflects primary productivity, which mostly includes endogenous plants in the lake, such as algae and aquatic plants (Kai et al., 2019).

The significant positive relationship between TOC and TN (R^2 = 0.98, p < 0.001; **Figure 5B**) observed for SY-2 core sediments suggests that TOC and TN are mainly autochthonous in the lake and that inorganic nitrogen from terrestrial materials is negligible (~0.05%) (e.g., Liu et al., 2009). Changes in TN indicate the nutritional status of the lake, which is strongly subject to changes in water temperature. Water temperature not only affects the change in TN but also directly and significantly affects the growth of plankton in lakes, thus changing the content of endogenous organic carbon (Lu and An, 2010). Therefore, the significant positive relationship between TOC and TN indicates that higher values of TOC and TN represent higher primary productivity and higher temperatures.

Mineralogy

For the lakes in the hinterland of the BJD, the lacustrine sediments were mainly from the aeolian deposits around the lakes (Li et al., 2018). The mineral compositions of surface sediments in lakes show that detrital minerals compose more than 90% and that the saline minerals in lakes are autochthonous (Suhui et al., 2015).

Authigenic carbonate deposition is related to many factors, such as temperature, salinity, and primary productivity within lakes (Kelts and Hsü, 1978; Tucker and Wright, 1990). In this study, the contents of organic matter and carbonate increased almost simultaneously. Due to the increased productivity, more CO_2 (aq) assimilation occurs by thriving algae photosynthesis

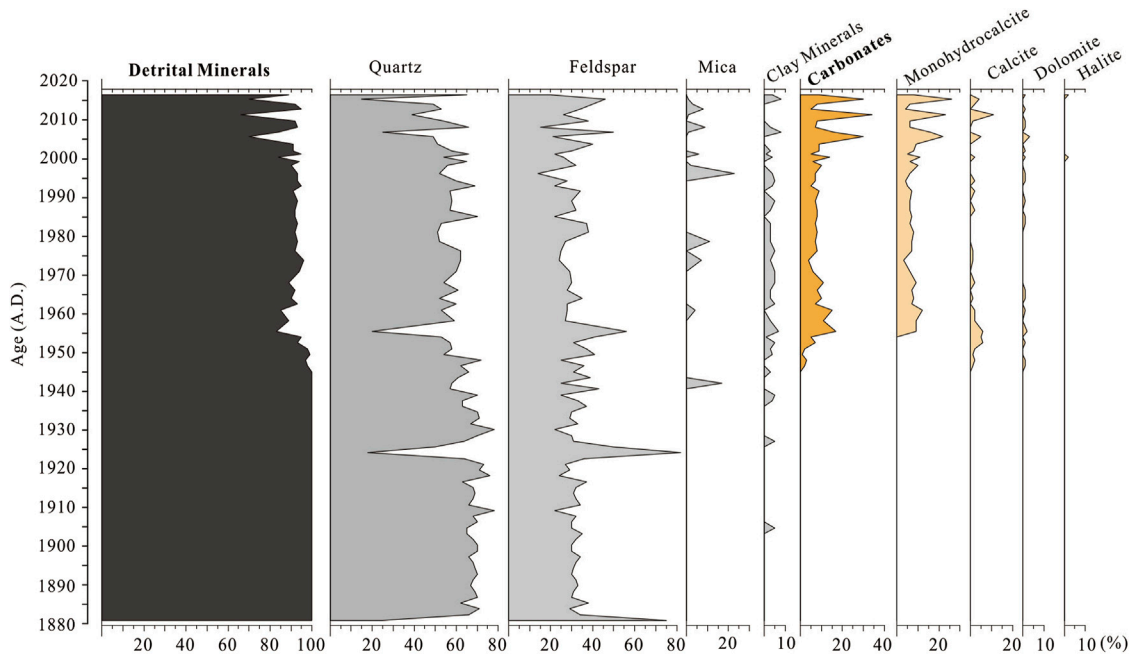

FIGURE 4 | Variations in mineral composition in core SY-2 from the BJD.

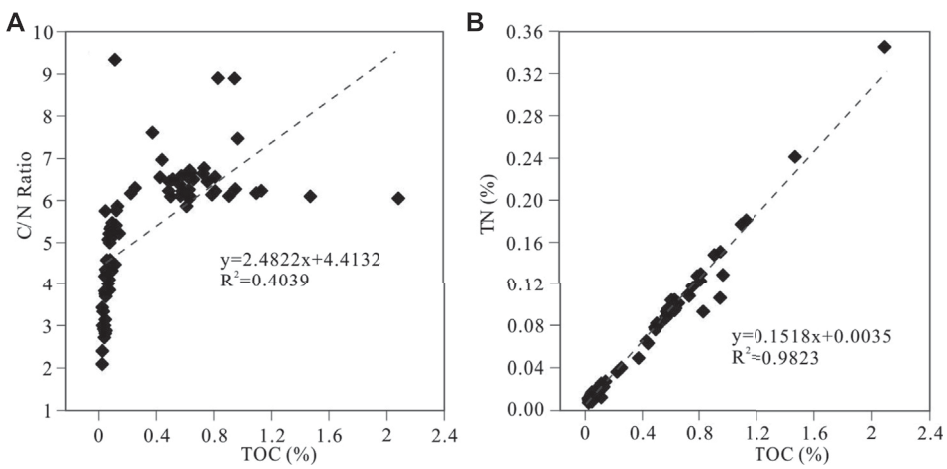

FIGURE 5 | Relationships of TOC content with C/N ratio and TN content in the SY-2 core.

(Opitz et al., 2012), leading to supersaturation of CO_3^{2-}, and promoting the deposition of carbonates via the reaction $2HCO_3^- \rightarrow CO_2$ (aq) + H_2O + CO_3^{2-} (Kelts and Hsü, 1978; Zhang et al., 2010). However, in the studied lake, the TOC and TN contents are very low, with average values of 0.77 and 0.13% in the 1950–2018 periods, respectively. This indicated that the primary productivity is very low compared to other lakes, such as Qinghai Lake (Chen et al., 2021) and Bosten Lake (Zhang et al., 2010). Therefore, the primary productivity may be minimal for carbonate precipitation.

Many previous studies suggest that salinity is the most important factor for carbonate precipitation in arid areas (Qiang et al., 2005; Wang et al., 2013; Li et al., 2016). The mineral composition of the surface sediments of the lakes in the BJD also indicated that the saline mineralogical composition and content in lake sediments vary with lake water salinity (Suhui et al., 2015). In core SY-2, the saline minerals are mainly carbonates, including monohydrocalcite, calcite, and dolomite. In the natural environment, monohydrocalcite is predominantly found in water with a high Mg/Ca ratio (high salinity) (Han et al.,

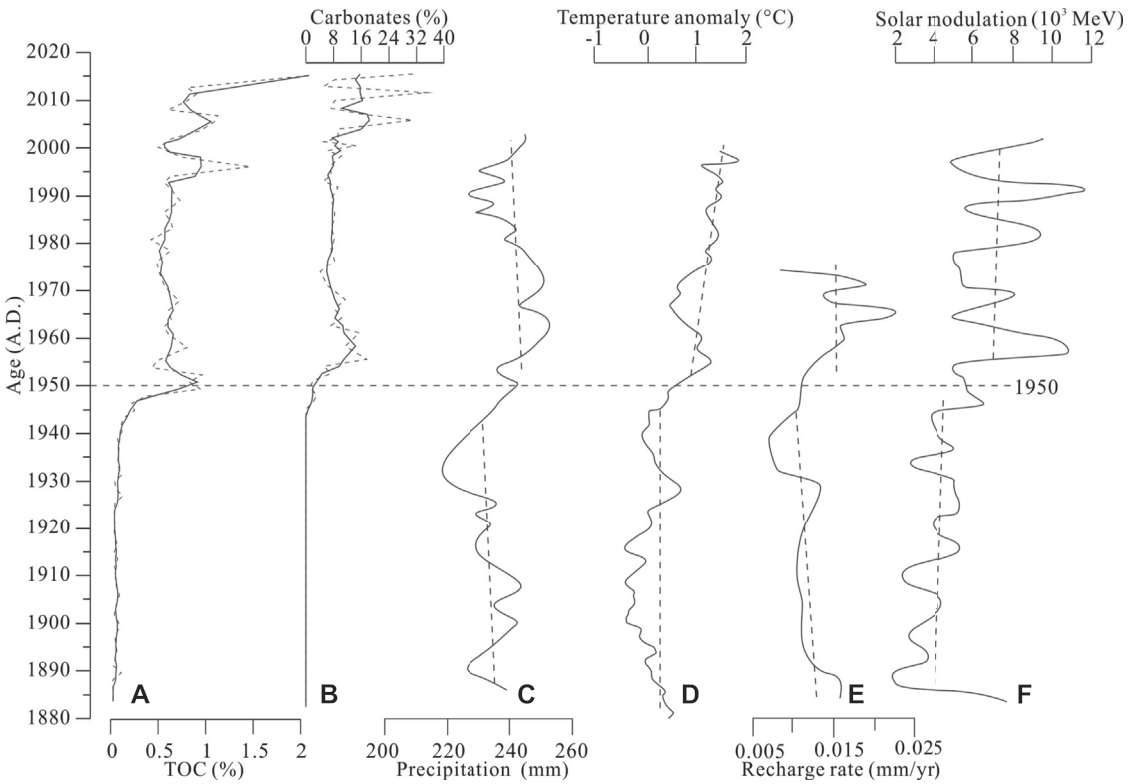

FIGURE 6 | TOC and carbonate contents of the SY-2 sedimentary core and comparisons with other regional climate records. **(A)-(B)** The TOC and carbonate contents of the SY-2 sedimentary core in this study. **(C)** Reconstruction of precipitation at the southern margin of the BJD (Zhang et al., 2015). **(D)** Temperature changes in Northwest China (Ding, 2010). **(E)** Recharge rate of the BJD (Gates et al., 2008b). **(F)** Solar activity (Muscheler et al., 2007).

2020), such as in the limestone of Ikka Fjord, Greenland (Mg/Ca > 5) (Dahl and Buchardt, 2006); Manito Lake sediments, Canada (Mg/Ca > 40) (Last, 2001); and Namco Lake sediments, Tibet (Mg/Ca > 10) (Li et al., 2009). High salinity, high Mg/Ca ratio, and high alkalinity in lake water facilitate the precipitation of dolomite (i.e., environments with high evaporation intensity) (Deckker and Last, 1988), and dolomite has also been considered an evaporative salt mineral in some studies (Qiang et al., 2005). Therefore, the carbonate content is regarded as an indicator of salinity in studies of lake change (Qiang et al., 2005; Wang et al., 2013).

Lake Evolution and Local Climate Records Over the Past 140 Years

Based on the TOC, TN, and carbonate mineral contents, the evolution of Sayinwusu Lake since 1880 can be divided into two periods. The first period dates from 1880 to 1950 (86–43 cm). During this period, the low contents of TOC and TN and predominantly detrital mineral composition indicate that the lake primary productivity and salinity were low (**Figures 6A,B**). The second period represents the time from 1950 to 2018 (above 43 cm). The contents of TOC, TN, and carbonate minerals increased rapidly at the beginning of the 1950s, indicating that the primary productivity and salinity of the lake increased (**Figures 6A,B**). Meanwhile, the simultaneous increases in TOC, TN, and carbonate minerals suggest an increase in regional temperature and evaporation effects. During the second period, the TOC, TN, and carbonate minerals were higher during 1955–1968 and 1998–2018, indicating relatively high temperatures and evaporation effects.

Due to the special geographical conditions, there have been a few studies on the reconstruction of regional climate and environment during the last several 100 years. A palynological study of Baoritaolegai Lake sediments in the southeastern BJD over the last 160 years identified three dry periods: the mid 1870s to the beginning of the 1900s, the beginning of the 1920s to the late 1930s, and the beginning of the 1960s to the present (Herzschuh et al., 2006). The tree rings of the shrub (*Zygophyllum xanthoxylum Maxim*) were affected by precipitation during the last 160 years, and three dry phases were identified: 1840s to early 1850s, early 1890s–1900s, and late 1970s to mid 1980s (Xiao et al., 2012). However, the salinity changes from the lake sediment archives in this study do not agree well with the climatic records of tree rings and palynology in the desert hinterland. There are two possible reasons for the differences. One explanation is that the local precipitation in the desert could not sustain the lakes (Ma et al., 2014). The lakes in the desert area are mainly recharged by groundwater, and the recharge source is from adjacent areas and/or other areas (e.g.,

Chen et al., 2004; Ma and Edmunds, 2006; Gates et al., 2008a; Shao et al., 2012; Dong et al., 2016; Wang et al., 2016). Similar to the groundwater recharge lakes in the Sahara Desert, lake evolution has little relevance in terms of the local climate but much pertinence regarding changes in groundwater recharge (Creutz et al., 2016). The other explanation is that the climate records of vegetation in the hinterland of the desert reflect precipitation before and during the vegetation growing season, especially the summer (Xiao et al., 2012). The hydrogen and oxygen isotopes of modern precipitation show that the precipitation in the desert is mainly from westerly moisture and that part of the summer is affected by the East Asian summer monsoon (Cao et al., 2020). Therefore, the climate reconstructed by vegetation records in desert areas is a mixed signal of westerly moisture and East Asian summer monsoon precipitation. Consequently, it is reasonable that there is no significant relationship between lake evolution and local precipitation in the BJD.

The Factors Influencing Lake Evolution

In this study, the simultaneous increases in TOC and TN contents indicate that the regional temperature rose at the beginning of the 1950s. Research integrating ice cores, stalagmites, and lake records reveals that the temperature of Northwest China warmed rapidly at the beginning of the 1950s (**Figure 6D**; Ding, 2010), which is consistent with the rapid warming trend in China (Ge et al., 2015). With rising temperatures, precipitation in the arid region of Northwest China has increased in recent decades (Chen et al., 2020; Liu et al., 2021). The reconstructed precipitation from tree rings shows that the annual precipitation began to increase at the beginning of the 1950s on the southern margin of the desert and the northeastern Tibetan Plateau (**Figure 6C**; Yang et al., 2010; Yang et al., 2014; Zhang et al., 2015; Liu et al., 2021). Although the recharge source of groundwater in the BJD is still controversial, previous studies have suggested that it is mainly the mountain areas in the southern BJD and/or the northern Tibetan Plateau (Chen et al., 2004; Ma and Edmunds, 2006; Gates et al., 2008a; Gates et al., 2008b; Dong et al., 2016). Therefore, the precipitation in recharge source areas has increased in recent decades. The recharge rate of groundwater in the southeastern BJD shows a high value after 1950 A.D. (Gates et al., 2008b), which indicates that the groundwater recharge amount of the lakes in the BJD increased (**Figure 6E**).

Although precipitation is important for lake evolution, evaporation is also an important control on the water balance, especially in arid and semiarid regions (Wu et al., 2020). Modern observations suggest that the evaporation of lakes is closely correlated with air temperature and water temperature in the BJD (Han et al., 2018). Due to the warm island effect of lakes in the BJD, the annual temperature in the lake group region is approximately 1.6°C higher than those in other regions (Liang et al., 2020), which may cause a more intense evaporation effect. When the enhancement of the evaporation effect caused by the temperature rise is much greater than the increased precipitation, the effective moisture decreases (Li et al., 2016; Wu et al., 2020). The salinization of lakes in the BJD at the beginning of the 1950s

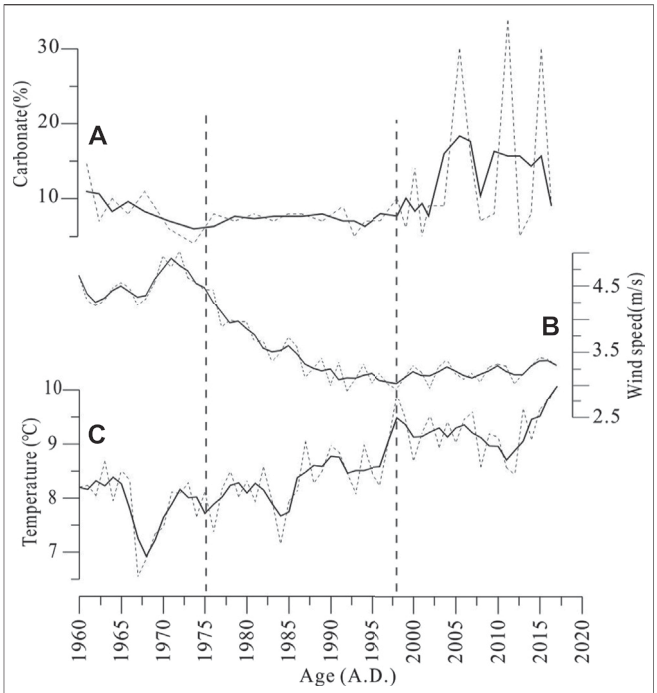

FIGURE 7 | Relationships between the carbonate contents of the SY-2 core **(A)** and the annual average temperature **(B)** and wind speed **(C)** during 1960–2017.

and the increased temperature simultaneously suggest that the increase in evaporation induced by the temperature rise was greater than that in groundwater recharge (Li et al., 2016; Wu et al., 2020). Wind speed is another important factor for evaporation. Due to the high sand mountains, the wind speed is low in the hinterland of the BJD (Ma and Wang, 2016). The carbonate content has no obvious relationship with the wind speed in the last 60 years but has good consistency with the temperature changes (**Figure 7**). This phenomenon is consistent with modern instrumental observations (Han et al., 2018).

Regionally, tree-ring records suggest that the last dry period was from the beginning of the 1950s to the present in the Hexi Corridor (Deng et al., 2017). In the long term, the drought periods in the Hexi Corridor tend to coincide with solar activity, which may be a possible external driving factor (**Figure 6F**; Muscheler et al., 2007; Deng et al., 2017). Several lakes in the northeastern Tibetan Plateau have also shown salinization resulting from high temperatures in recent decades, such as Hala Lake (Cao et al., 2007), Sugan Lake (Chen et al., 2009), and Qinghai Lake (Zhang et al., 2004). Furthermore, dry basins or shrinking lakes in the geological period also occurred under the high temperature and precipitation climate in the northeastern Tibetan Plateau and Hexi Corridor (Liu et al., 2013; Wang et al., 2014; Wu et al., 2020). Therefore, for other areas of the world, although there are differences in the timing of temperature increases, they all lead to droughts and extreme events (Hegerl et al., 2018; Neukom et al., 2019; Woolway et al., 2020; Che et al., 2021).

In the context of global warming (Neukom et al., 2019), lake surface water temperatures have increased worldwide at a global

average rate of 0.34°C decade^{-1}, and global annual mean lake evaporation rates are forecast to increase 16% by 2,100 relative to 2006–2015 (Woolway et al., 2020). Arid zones are more sensitive than other areas to temperature changes during global climate change, especially desert areas (Chen et al., 2015; Huang et al., 2016; Liang et al., 2020). Remote sensing data show that the lake areas in the BJD and central Asia have decreased in recent decades (Zhang et al., 2013; Che et al., 2021). With ongoing global warming, our results suggest that lakes in arid areas, especially in desert areas, will become increasingly salty, and this issue should have been addressed earlier.

CONCLUSION

^{210}Pb and ^{137}Cs dating, TOC, TN, and mineral content analysis were used to reconstruct the lake hydrological changes during the past 140 years. From 1880 to 1950, the primary productivity and salinity of Sayinwusu Lake were low. From 1950 to 2018, the TOC, TN, and carbonate minerals increased rapidly at the beginning of the 1950s, indicating that the primary productivity and salinity of the lake increased.

At the beginning of the 1950s, the TOC and TN contents increased synchronously, indicating increases in primary productivity and temperature. Regional climate reconstruction data also suggest that precipitation and temperature have increased in recent decades. However, the enhancement of the evaporation effect caused by the temperature rise is much greater than the increased precipitation in arid areas, especially in desert areas.

DATA AVAILABILITY STATEMENT

The original contributions presented in the study are included in the article/Supplementary Material; further inquiries can be directed to the corresponding authors.

AUTHOR CONTRIBUTIONS

All authors listed have made substantial, direct, and intellectual contributions to the work and approved it for publication.

FUNDING

This research was financially supported by the National Natural Science Foundation of China (41807420 and 41871021), the National Key R and D Programme of China (No. 2019YFC0409201), the project of the China Geological Survey (121201106000150093) and the Basic Research Programme of Institute of Hydrogeology and Environmental Geology, Chinese Academy of Geological Sciences (CAGS) (SK202007).

ACKNOWLEDGMENTS

We are grateful to Li Zhuolun at Lanzhou University and Le Cao, Pucheng Zhu, Jinsong Yang, Dejun Wan, Kai Ning, Min Liu, and other colleagues at the Institute of Hydrogeology and Environmental Geology, CAGS, who have contributed to our field work and data analysis.

REFERENCES

Appleby, P. G. (2001). "Chronostratigraphic Techniques in Recent Sediments," in *Tracking Environmental Change Using Lake Sediments: Basin Analysis, Coring, and Chronological Techniques*. Editors W.M. Last and J.P. Smol (Dordrecht, Netherlands: Springer Netherlands), 171–203.

Appleby, P. G., and Oldfield, F. (1978). The Calculation of Lead-210 Dates Assuming a Constant Rate of Supply of Unsupported 210Pb to the Sediment. *Catena.* 5, 1–8. doi:10.1016/s0341-8162(78)80002-2

Audry, S., Schäfer, J., Blanc, G., and Jouanneau, J.-M. (2004). Fifty-Year Sedimentary Record of Heavy Metal Pollution (Cd, Zn, Cu, Pb) in the Lot River Reservoirs (France). *Environ. Pollut.* 132, 413–426. doi:10.1016/j.envpol.2004.05.025

Bai, Y., Wang, N. A., He, R. X., Li, J. M., and Lai, Z. P. (2011). Ground Penetrating Radar Images and Optically Stimulated Luminescence Dating for Lacustrine Deposition of the Badain Jaran Desert. *J. Desert Res.* 31, 842–847.

BGMIMAR (Bureau of Geology Mineral Resources of Inner Mongolia Autonomous Region) (1991). *Regional Geology of Inner Mongolia Autonomous Region*. Beijing, China: Geological Publishing House.

Cao, J., Zhang, J. W., Zhang, C. J., and Chen, F. H. (2007). Environmental Changes During the Past 800 Years Recorded in Lake Sediments From Hala Lake on the Northern Tibetan Plateau. *Quat. Sci.* 27, 100–107.

Cao, L., Shen, J. M., Nie, Z. L., Meng, L. Q., Liu, M., and Wang, Z. (2020). Stable Isotopic Characteristics of Precipitation and Moisture Recycling in the Badain Jaran Desert. *Earth Sci.* doi:10.3799/dqkx.2020.273

Che, X., Feng, M., Sun, Q., Sexton, J. O., Channan, S., and Liu, J. (2021). The Decrease in Lake Numbers and Areas in Central Asia Investigated Using a Landsat-Derived Water Dataset. *Remote Sensing.* 13, 1032. doi:10.3390/rs13051032

Chen, C., Zhang, X., Lu, H., Jin, L., Du, Y., and Chen, F. (2020). Increasing Summer Precipitation in Arid Central Asia Linked to the Weakening of the East Asian Summer Monsoon in the Recent Decades. *Int. J. Climatol.* 41, 1024–1038. doi:10.1002/joc.6727

Chen, J., Chen, F., Zhang, E., Brooks, S. J., Zhou, A., and Zhang, J. (2009). A 1000-Year Chironomid-Based Salinity Reconstruction From Varved Sediments of Sugan Lake, Qaidam Basin, Arid Northwest China, and its Palaeoclimatic Significance. *Chin. Sci. Bull.* 54, 3749–3759. doi:10.1007/s11434-009-0201-8

Chen, J. S., Li, L., Wang, J. Y., Barry, D. A., Sheng, X. F., Gu, W. Z., et al. (2004). Groundwater Maintains Dune Landscape. *Nature.* 432, 459–460. doi:10.1038/432459a

Chen, T., Lai, Z., Liu, S., Wang, Y., Wang, Z.-t., Miao, X., et al. (2019). Luminescence Chronology and Palaeoenvironmental Significance of Limnic Relics From the Badain Jaran Desert, Northern China. *J. Asian Earth Sci.* 177, 240–249. doi:10.1016/j.jseaes.2019.03.024

Chen, X., Meng, X., Song, Y., Zhang, B., Wan, Z., Zhou, B., et al. (2021). Spatial Patterns of Organic and Inorganic Carbon in Lake Qinghai Surficial Sediments and Carbon Burial Estimation. *Front. Earth Sci.* 9. doi:10.3389/feart.2021.714936

Chen, Y., Li, Z., Fan, Y., Wang, H., and Deng, H. (2015). Progress and Prospects of Climate Change Impacts on Hydrology in the Arid Region of Northwest China. *Environ. Res.* 139, 11–19. doi:10.1016/j.envres.2014.12.029

Creutz, M., Van Bocxlaer, B., Abderamane, M., and Verschuren, D. (2016). Recent Environmental History of the Desert Oasis Lakes at Ounianga Serir, Chad. *J. Paleolimnol.* 55, 167–183. doi:10.1007/s10933-015-9874-y

Cui, X. J., Dong, Z. B., Lu, J. F., Wang, M., Li, J. Y., and Luo, W. Y. (2014). Relationship Between Vegetation Feature and Physiognomy Morphology of Mega-Dunes in Badain Jaran Desert. *Bull. Soil Water Conserv.* 34, 278–283.

Dahl, K., and Buchardt, B. (2006). Monohydrocalcite in the Arctic Ikka Fjord, SW Greenland: First Reported Marine Occurrence. *J. Sediment. Res.* 76, 460–471. doi:10.2110/jsr.2006.035

Deckker, P. D., and Last, W. M. (1988). Modern Dolomite Deposition in Continental, Saline Lakes, Western Victoria, Australia. *Geology.* 16, 29. doi:10.1130/0091-7613(1988)016<0029:mddics>2.3.co;2

Deng, Y., Gou, X., Gao, L., Yang, M., and Zhang, F. (2017). Tree-Ring Recorded Moisture Variations Over the Past Millennium in the Hexi Corridor, Northwest China. *Environ. Earth Sci.* 76, 272. doi:10.1007/s12665-017-6581-1

Ding, Z. L. (2010). *Integrated Study on Environmental Evolution in Western China*. Meteorological Press.

Dong, C., Wang, N. a., Chen, J., Li, Z., Chen, H., Chen, L., et al. (2016). New Observational and Experimental Evidence for the Recharge Mechanism of the Lake Group in the Alxa Desert, north-central China. *J. Arid Environments.* 124, 48–61. doi:10.1016/j.jaridenv.2015.07.008

Dong, S., Li, Z., Chen, Q., and Wei, Z. (2018). Total Organic Carbon and its Environmental Significance for the Surface Sediments in Groundwater Recharged Lakes From the Badain Jaran Desert, Northwest China. *J. Limnol.* 77, 121–129. doi:10.4081/jlimnol.2017.1667

Dong, Z., Qian, G., Lv, P., and Hu, G. (2013). Investigation of the Sand Sea With the Tallest Dunes on Earth: China's Badain Jaran Sand Sea. *Earth-Science Rev.* 120, 20–39. doi:10.1016/j.earscirev.2013.02.003

Dong, Z., Wang, T., and Wang, X. (2004). Geomorphology of the Megadunes in the Badain Jaran Desert. *Geomorphology.* 60, 191–203. doi:10.1016/j.geomorph.2003.07.023

Fu, C., Wu, H., Zhu, Z., Song, C., Xue, B., Wu, H., et al. (2021). Exploring the Potential Factors on the Striking Water Level Variation of the Two Largest Semi-Arid-Region Lakes in Northeastern Asia. *Catena.* 198, 105037. doi:10.1016/j.catena.2020.105037

Gates, J. B., Edmunds, W. M., Darling, W. G., Ma, J., Pang, Z., and Young, A. A. (2008a). Conceptual Model of Recharge to Southeastern Badain Jaran Desert Groundwater and Lakes From Environmental Tracers. *Appl. Geochem.* 23, 3519–3534. doi:10.1016/j.apgeochem.2008.07.019

Gates, J. B., Edmunds, W. M., Jinzhu Ma, M., and Sheppard, P. R. (2008b). A 700-Year History of Groundwater Recharge in the Drylands of NW China. *The Holocene.* 18, 1045–1054. doi:10.1177/0959683608095575

Ge, Q. S., Zheng, J. Y., and Hao, Z. X. (2015). PAGES Synthesis Study on Climate Changes in Asia over the Last 2000 years: Progresses and Perspectives. *Acta Geogr. Sin.* 70, 355–363.

Han, L., Li, Y., Liu, X., and Yang, H. (2020). Paleoclimatic Reconstruction and the Response of Carbonate Minerals During the Past 8000 Years Over the Northeast Tibetan Plateau. *Quat. Int.* 553, 94–103. doi:10.1016/j.quaint.2020.06.009

Han, P. F., Wang, X. S., Hu, X. N., Jiang, X. W., and Zhou, Y. Y. (2018). Dynamic Relationship Between Lake Surface Evaporation and Meterorological Factors in the Badian Jaran Desert. *Arid Zone Res.* 35, 1013–1020.

Hedges, J. I., Baldock, J. A., Gélinas, Y., Lee, C., Peterson, M. L., and Wakeham, S. G. (2002). The Biochemical and Elemental Compositions of Marine Plankton: a NMR Perspective. *Mar. Chem.* 78, 47–63. doi:10.1016/s0304-4203(02)00009-9

Hegerl, G. C., Brönnimann, S., Schurer, A., and Cowan, T. (2018). The Early 20th Century Warming: Anomalies, Causes, and Consequences. *Wires Clim. Change.* 9, e522. doi:10.1002/wcc.522

Herzschuh, U., Kürschner, H., Battarbee, R., and Holmes, J. (2006). Desert Plant Pollen Production and a 160-Year Record of Vegetation and Climate Change on the Alashan Plateau, NW China. *Veget Hist. Archaeobot.* 15, 181–190. doi:10.1007/s00334-005-0031-9

Hu, F., and Yang, X. (2016). Geochemical and Geomorphological Evidence for the Provenance of Aeolian Deposits in the Badain Jaran Desert, Northwestern China. *Quat. Sci. Rev.* 131, 179–192. doi:10.1016/j.quascirev.2015.10.039

Hu, W. F., Wang, N. A., Zhao, L. Q., Ning, K., Zhang, H. X., and Sun, J. (2015). Water-Heat Exchange Over a Typical Lake in Badain Jaran Desert, China. *Prog. Geogr.* 34, 1061–1071.

Huang, J., Yu, H., Guan, X., Wang, G., and Guo, R. (2016). Accelerated Dryland Expansion Under Climate Change. *Nat. Clim Change.* 6, 166–171. doi:10.1038/nclimate2837

Jin, Z., Han, Y., and Chen, L. (2010). Past Atmospheric Pb Deposition in Lake Qinghai, Northeastern Tibetan Plateau. *J. Paleolimnol.* 43, 551–563. doi:10.1007/s10933-009-9351-6

Kai, N., Naiang, W., Xiaonan, L., Zhuolun, L., Jiaqi1, S., Ran, A., et al. (2019). A Grain Size and N-Alkanes Record of Holocene Environmental Evolution From a Groundwater Recharge Lake in Badain Jaran Desert, Northwestern China. *The Holocene.* 29, 1045–1058. doi:10.1177/0959683619831430

Kelts, K., and Hsü, K. J. (1978). "Freshwater Carbonate Sedimentation," in *Lakes: Chemistry, Geology, Physics*. Editor A. Lerman (New York: Springer-Verlag), 295–323. doi:10.1007/978-1-4757-1152-3_9

Last, W. M. (2001). "Tracking Environmental Change Using lake Sediments: Physical and Geochemical Methods," in *Mineralogical Analysis of Lake Sediments*. Editor W.M. Last (Last (Netherlands: Springer), 143–187.

Li, M., Kang, S., Zhu, L., Wang, F., Wang, J., Yi, C., et al. (2009). On the Unusual Holocene Carbonate Sediment in Lake Nam Co, Central Tibet. *J. Mt. Sci.* 6, 346–353. doi:10.1007/s11629-009-1020-8

Li, Z., Wang, N. a., Cheng, H., and Li, Y. (2016). Early-Middle Holocene Hydroclimate Changes in the Asian Monsoon Margin of Northwest China Inferred From Huahai Terminal lake Records. *J. Paleolimnol.* 55, 289–302. doi:10.1007/s10933-016-9880-8

Li, Z., Wei, Z., Dong, S., and Chen, Q. (2018). The Paleoenvironmental Significance of Spatial Distributions of Grain Size in Groundwater-Recharged Lakes: A Case Study in the Hinterland of the Badain Jaran Desert, Northwest China. *Earth Surf. Process. Landforms.* 43, 363–372. doi:10.1002/esp.4248

Liang, X., Zhao, L., Xu, X., Niu, Z., Zhang, W., and Wang, N. a. (2020). Plant Phenological Responses to the Warm Island Effect in the Lake Group Region of the Badain Jaran Desert, Northwestern China. *Ecol. Inform.* 57, 101066. doi:10.1016/j.ecoinf.2020.101066

Liu, S., NarentuyaXia, B., Xia, G., and Tian, M. (2012). Using 210Pbuns and 137Cs to Date Recent Sediment Cores From the Badain Jaran Desert, Inner Mongolia, China. *Quat. Geochronol.* 12, 30–39. doi:10.1016/j.quageo.2012.06.001

Liu, S. W., Chu, G. Q., and Lai, Z. P. (2016). Determination of Age and Sedimentation Rates Using Radionuclide (210Pbuns and 137Cs) Dating in Inter-Dune Lakes of the Badain Jaran Desert, China. *Acta Geol. Sin.* 90, 2013–2022.

Liu, W., Gou, X., Li, J., Huo, Y., Yang, M., Zhang, J., et al. (2021). Temperature Signals Complicate Tree-Ring Precipitation Reconstructions on the Northeastern Tibetan Plateau. *Glob. Planet. Change.* 200, 103460. doi:10.1016/j.gloplacha.2021.103460

Liu, W., Li, X., An, Z., Xu, L., and Zhang, Q. (2013). Total Organic Carbon Isotopes: a Novel Proxy of Lake Level From Lake Qinghai in the Qinghai-Tibet Plateau, China. *Chem. Geology.* 347, 153–160. doi:10.1016/j.chemgeo.2013.04.009

Liu, X., Dong, H., Yang, X., Herzschuh, U., Zhang, E., Stuut, J.-B. W., et al. (2009). Late Holocene Forcing of the Asian Winter and Summer Monsoon as Evidenced by Proxy Records From the Northern Qinghai-Tibetan Plateau. *Earth Planet. Sci. Lett.* 280, 276–284. doi:10.1016/j.epsl.2009.01.041

Long, H., Lai, Z., Fuchs, M., Zhang, J., and Li, Y. (2012). Timing of Late Quaternary Palaeolake Evolution in Tengger Desert of Northern China and its Possible Forcing Mechanisms. *Glob. Planet. Change.* 92-93, 119–129. doi:10.1016/j.gloplacha.2012.05.014

Lopez, L. S., Hewitt, B. A., and Sharma, S. (2019). Reaching a Breaking point: How Is Climate Change Influencing the Timing of Ice Breakup in Lakes Across the Northern Hemisphere? *Limnol. Oceanogr.* 64, 2621–2631. doi:10.1002/lno.11239

Lu, F. Y., and An, Z. S. (2010). Pretreatment Methods for Analyzing the Total Organic Carbon and Nitrogen Contents of Heqing Core Sediments and Their Environmental Significances. *J. Geomech.* 46, 393–401.

Lu, Y., Wang, N. A., Li, G. P., Li, Z. L., Dong, C. Y., and Lu, J. W. (2010). Spatial Distribution of Lakes Hydro-Chemical Types in Badain Jaran Desert. *J. Lake Sci.* 22, 774–782.

Ma, J., and Edmunds, W. M. (2006). Groundwater and Lake Evolution in the Badain Jaran Desert Ecosystem, Inner Mongolia. *Hydrogeol. J.* 14, 1231–1243. doi:10.1007/s10040-006-0045-0

Ma, N., and Wang, N. A. (2016). On the Simulation of Evaporation From Lake Surface in the Hinterland of the Badain Jaran Desert. *Arid Zone Res.* 33, 1141–1149.

Ma, N., Wang, N., Zhao, L., Zhang, Z., Dong, C., and Shen, S. (2014). Observation of Mega-Dune Evaporation after Various Rain Events in the Hinterland of Badain Jaran Desert, China. *Chin. Sci. Bull.* 59, 162–170. doi:10.1007/s11434-013-0050-3

Meyers, P. A. (2003). Applications of Organic Geochemistry to Paleolimnological Reconstructions: a Summary of Examples From the Laurentian Great Lakes. *Org. Geochem.* 34, 261–289. doi:10.1016/s0146-6380(02)00168-7

Mischke, S. (2005). New Evidence for Origin of Badain Jaran Desert of Inner Mongoliafrom Granulometry and Thermoluminescence Dating. *J. Palaeogeogr.* 7, 79–97.

Muscheler, R., Joos, F., Beer, J., Müller, S. A., Vonmoos, M., and Snowball, I. (2007). Solar Activity During the Last 1000yr Inferred From Radionuclide Records. *Quat. Sci. Rev.* 26, 82–97. doi:10.1016/j.quascirev.2006.07.012

Neukom, R., Steiger, N., Gómez-Navarro, J. J., Wang, J., and Werner, J. P. (2019). No Evidence for Globally Coherent Warm and Cold Periods Over the

Preindustrial Common Era. *Nature.* 571, 550–554. doi:10.1038/s41586-019-1401-2

Ning, W. X., Liu, X. Y., and Wang, Z. T. (2021). Temperature and Precipitation Characteristics and Spatial Stratified Heterogeneity in Badain Jaran Desert. *J. Univ. Chin. Acad. Sci.* 38, 103–113.

Opitz, S., Wünnemann, B., Aichner, B., Dietze, E., Hartmann, K., Herzschuh, U., et al. (2012). Late Glacial and Holocene Development of Lake Donggi Cona, North-Eastern Tibetan Plateau, Inferred From Sedimentological Analysis. *Palaeogeogr. Palaeoclimatol. Palaeoecol.* 337-338, 159–176. doi:10.1016/j.palaeo.2012.04.013

Panizzo, V. N., Mackay, A. W., Rose, N. L., Rioual, P., and Leng, M. J. (2013). Recent Palaeolimnological Change Recorded in Lake Xiaolongwan, Northeast China: Climatic versus Anthropogenic Forcing. *Quat. Int.* 290-291, 322–334. doi:10.1016/j.quaint.2012.07.033

Qiang, M., Chen, F., Zhang, J., Gao, S., and Zhou, A. (2005). Climatic Changes Documented by Stable Isotopes of Sedimentary Carbonate in Lake Sugan, Northeastern Tibetan Plateau of China, since 2 kaBP. *Chin. Sci Bull.* 50, 1930–1939. doi:10.1360/04wd0285

Robbins, J. A., and Edgington, D. N. (1975). Determination of Recent Sedimentation Rates in Lake Michigan Using Pb-210 and Cs-137. *Geochimica et Cosmochimica Acta.* 39, 285–304. doi:10.1016/0016-7037(75)90198-2

Shao, T., Zhao, J., Zhou, Q., Dong, Z., and Ma, Y. (2012). Recharge Sources and Chemical Composition Types of Groundwater and Lake in the Badain Jaran Desert, Northwestern China. *J. Geogr. Sci.* 22, 479–496. doi:10.1007/s11442-012-0941-2

Suhui, M., Li, Z. L., Zhuolun, L., Naiang, W., Kai, N., and Meng, L. (2015). Mineralogical Assemblages in Surface Sediments and its Formation Mechanism in the Groundwater Recharged Lakes: a Case Study of Lakes in the Badain Jaran Desert. *J. Lake Sci.* 27, 727–734. doi:10.18307/2015.0422

Swarzenski, P. W. (2014). "210Pb Dating," in *Encyclopedia of Scientific Dating Methods*. Editors W. J. Rink and J. Thompson (Dordrecht, Netherlands: Springer Netherlands), 1–11. doi:10.1007/978-94-007-6326-5_236-1

Tucker, M. E., and Wright, V. P. (1990). "Carbonate Mineralogy and Chemistry," in *Carbonate Sedimentology*. Editors M. E. Tucker and V. P. Wright (Oxford, UK: Blackwell Science), 284–313.

Wan, D., Mao, X., Jin, Z., Song, L., Yang, J., and Yang, H. (2019). Sedimentary Biogeochemical Record in Lake Gonghai: Implications for Recent Lake Changes in Relatively Remote Areas of China. *Sci. Total Environ.* 649, 929–937. doi:10.1016/j.scitotenv.2018.08.331

Wang, F., Li, Z., Wang, X., Li, B., and Chen, F. (2018). Variation and Interplay of the Siberian High and Westerlies in Central-East Asia During the Past 1200kyr. *Aeolian Res.* 33, 62–81. doi:10.1016/j.aeolia.2018.05.003

Wang, F., Sun, D., Chen, F., Bloemendal, J., Guo, F., Li, Z., et al. (2015a). Formation and Evolution of the Badain Jaran Desert, North China, as Revealed by a Drill Core from the Desert centre and by Geological Survey. *Palaeogeogr. Palaeoclimatol. Palaeoecol.* 426, 139–158. doi:10.1016/j.palaeo.2015.03.011

Wang, M., Dong, Z., Luo, W., Lu, J., Li, J., Cui, X., et al. (2015b). Species Diversity of Vegetation and its Relationship With Soil Characteristics in the Southern Marginal Zone of the Badain Jaran Desert. *Acta Bot. Boreal. – Occident. Sin.* 35, 379–388.

Wang, H., Dong, H., Zhang, C. L., Jiang, H., Zhao, M., Liu, Z., et al. (2014). Water Depth Affecting Thaumarchaeol Production in Lake Qinghai, Northeastern Qinghai-Tibetan Plateau: Implications for Paleo Lake Levels and Paleoclimate. *Chem. Geology.* 368, 76–84. doi:10.1016/j.chemgeo.2014.01.009

Wang, N. a., Li, Z., Li, Y., and Cheng, H. (2013). Millennial-Scale Environmental Changes in the Asian Monsoon Margin During the Holocene, Implicated by the Lake Evolution of Huahai Lake in the Hexi Corridor of Northwest China. *Quat. Int.* 313-314, 100–109. doi:10.1016/j.quaint.2013.08.039

Wang, N., Ning, K., Li, Z., Wang, Y., Jia, P., and Ma, L. (2016). Holocene High Lake-Levels and Pan-Lake Period on Badain Jaran Desert. *Sci. China Earth Sci.* 59, 1633–1641. doi:10.1007/s11430-016-5307-7

Woolway, R. I., Kraemer, B. M., Lenters, J. D., Merchant, C. J., O'Reilly, C. M., and Sharma, S. (2020). Global Lake Responses to Climate Change. *Nat. Rev. Earth Environ.* 1, 388–403. doi:10.1038/s43017-020-0067-5

Wu, D., Zhou, A., Zhang, J., Chen, J., Li, G., Wang, Q., et al. (2020). Temperature-Induced Dry Climate in Basins in the Northeastern Tibetan Plateau During the Early to Middle Holocene. *Quat. Sci. Rev.* 237, 106311. doi:10.1016/j.quascirev.2020.106311

Xiao, S. C., Xiao, H. L., Dong, Z. B., and Peng, X. M. (2012). Dry/wet Variation Recorded by Shrub Tree-Rings in the Central Badain Jaran Desert of Northwestern China. *J. Arid Environments.* 87, 85–94. doi:10.1016/j.jaridenv.2012.06.013

Yan, M., Wang, G., Li, B., and Dong, G. (2001). Formation and Growth of High Mega-Dunes in Badain Jaran Desert. *Acta Geogr. Sin.* 56, 83–91.

Yang, B., Qin, C., Wang, J., He, M., Melvin, T. M., Osborn, T. J., et al. (2014). A 3,500-Year Tree-Ring Record of Annual Precipitation on the Northeastern Tibetan Plateau. *Proc. Natl. Acad. Sci.* 111, 2903–2908. doi:10.1073/pnas.1319238111

Yang, X. (1991). Geomorphologische Untersuchungen in Trockenräumen NW-Chinas Unter Besonderer Berücksichtigung von Badanjilin und Takelamagan. *Gött. Geogr. Abh.* 96, 1–124.

Yang, X., Ma, N., Dong, J., Zhu, B., Xu, B., Ma, Z., et al. (2010). Recharge to the Inter-Dune Lakes and Holocene Climatic Changes in the Badain Jaran Desert, Western China. *Quat. Res.* 73, 10–19. doi:10.1016/j.yqres.2009.10.009

Yang, X., Scuderi, L., Paillou, P., Liu, Z., Li, H., and Ren, X. (2011). Quaternary Environmental Changes in the Drylands of China - A Critical Review. *Quat. Sci. Rev.* 30, 3219–3233. doi:10.1016/j.quascirev.2011.08.009

Yang, X., and Williams, M. A. J. (2003). The Ion Chemistry of Lakes and Late Holocene Desiccation in the Badain Jaran Desert, Inner Mongolia, China. *Catena.* 51, 45–60. doi:10.1016/S0341-8162(02)00088-7

Zhai, D., Xiao, J., Zhou, L., Wen, R., Chang, Z., Wang, X., et al. (2011). Holocene East Asian Monsoon Variation Inferred From Species Assemblage and Shell Chemistry of the Ostracodes from Hulun Lake, Inner Mongolia. *Quat. Res.* 75, 512–522. doi:10.1016/j.yqres.2011.02.008

Zhang Chengjun, C., Feng Zhaodong, Z., Yang Qili, Q., Gou Xiaohui, X., and Sun Feifei, F. (2010). Holocene Environmental Variations Recorded by Organic-Related and Carbonate-Related Proxies of the Lacustrine Sediments from Bosten Lake, Northwestern China. *The Holocene.* 20, 363–373. doi:10.1177/0959683609353428

Zhang, E., Shen, J., Wang, S., Yin, Y., Zhu, Y., and Xia, W. (2004). Quantitative Reconstruction of the Paleosalinity at Qinghai Lake in the Past 900 Years. *Chin.Sci.Bull.* 49, 730–734. doi:10.1007/BF03184273

Zhang, X. B., Long, Y., Wen, A. B., and He, X. B. (2012). Discussion on Applying 137Cs and 210Pbex for Lake Sediment Dating in China. *Quat. Sci.* 32, 430–440.

Zhang, Y. X., Yu, L., and Yin, H. (2015). Annual Precipitation Reconstruction Over Last 191 Years at the South Edge of Badain Jaran Desert Based on Tree Ring Width Data. *Desert Oasis Meteorol.* 9, 12–16.

Zhang, Z. G., and Li, L. R. (2005a). *Groundwater Resource of China (Gansu Vol).* Peking, China: Sino Maps Press.

Zhang, Z. G., and Li, L. R. (2005b). *Groundwater Resource of China (Xinjiang Vol).* Peking, China: Sino Maps Press.

Zhenyu, Z., Wang, N. A., Nai'ang, W., Yue, W., Shiping, S., Xunhe, Z., et al. (2013). Remote Sensing on Spatial Changes of Lake Area in Badain Jaran Desert Hinterland during 1973 2010. *J. Lake Sci.* 25, 514–520. doi:10.18307/2013.0408

Zhu, J., Wang, N. A., Chen, H. B., Dong, C., and Zhang, H. A. (2010). Study on the Boundary and the Area of Badain Jaran Desert Based on Remote Sensing Imagery. *Prog. Geogr.* 29, 1087–1094.

Conflict of Interest: The authors declare that the research was conducted in the absence of any commercial or financial relationships that could be construed as a potential conflict of interest.

Publisher's Note: All claims expressed in this article are solely those of the authors and do not necessarily represent those of their affiliated organizations, or those of the publisher, the editors and the reviewers. Any product that may be evaluated in this article, or claim that may be made by its manufacturer, is not guaranteed or endorsed by the publisher.